THE ROYAL SOCIETY

Received 14 February 2003
Accepted 12 March 2003
Published online 10 June 2003

Nanostructure predicts intraspecific variation in ultraviolet-blue plumage colour†

Matthew D. Shawkey*, Anne M. Estes†, Lynn M. Siefferman and Geoffrey E. Hill

Department of Biological Sciences, Auburn University, 331 Funchess Hall, Auburn, AL 36849, USA

Evidence suggests that structural plumage colour can be an honest signal of individual quality, but the mechanisms responsible for the variation in expression of structural coloration within a species have not been identified. We used full-spectrum spectrometry and transmission electron microscopy to investigate the effect of variation in the nanostructure of the spongy layer on expression of structural ultraviolet (UV)–blue coloration in eastern bluebird (*Sialia sialis*) feathers. Fourier analysis revealed that feather nanostructure was highly organized but did not accurately predict variation in hue. Within the spongy layer of feather barbs, the number of circular keratin rods significantly predicted UV–violet chroma, whereas the standard error of the diameter of these rods significantly predicted spectral saturation. These observations show that the precision of nanostructural arrangement determines some colour variation in feathers.

Keywords: structural colour; feather nanostructure; sexual selection; Fourier analysis

1. INTRODUCTION

Ultraviolet (UV)–blue structural plumage colour is largely a function of the size and arrangement of keratin rods and air spaces in the spongy medullary layer of feather barbs (Gadow 1882; Dyck 1971*a*,*b*; Prum *et al.* 1998, 1999*a*). Until recently, it had been thought that the reflective properties of spongy tissue were explained by incoherent Rayleigh (Häcker & Meyer 1902) or Mie (Finger 1995) scattering (reviewed in Prum 1999), in which the phase relationships among the scattered lightwaves are random. These models predict that the arrangement of scatterers (i.e. keratin rods and air spaces) is random and that scatterers of the small size found in spongy tissue scatter shorter wavelengths of light more efficiently than longer wavelengths.

Models of coherent scattering propose that the spongy layer can produce differential propagation of light waves as a result of the interactions among the scattered waves. By these models, the colour observed is the *sum* of the waves scattered by the array, rather than the result of differential scattering of some wavelengths. Dyck (1971*a*,*b*), in his 'hollow cylinder model', postulated that the sizes of keratin bars and air spaces in the spongy layer allow constructive interference and coherent scattering of light waves to produce colours. This model was supported by the findings of Prum *et al.* (1998, 1999*a*) that the spongy layer is not randomly organized and is, in fact, highly structured and appropriately scaled to produce the observed colours by constructive interference.

Despite substantial interest in the signal content of structural coloration (e.g. Bennett *et al.* 1997; Andersson *et al.* 1998; Keyser & Hill 1999), no study has sought associations between colour and nanostructural variables among individuals within a population. We use full-spectrum spectrometry and transmission electron microscopy (TEM) to investigate the effect of variation in spongy layer nanostructure on colour in eastern bluebird (*Sialia sialis*) feathers.

2. MATERIAL AND METHODS

(a) *Sampling*

We captured 30 adult male bluebirds in Lee County, Alabama, USA (32°35′ N, 82°28′ W), in June 2002. We pulled 8–12 feathers from the same area on the rump of each bird and stored them in small manila envelopes in a climate-controlled room until the time of analysis.

(b) *Spectrometry*

We taped feathers to black construction paper and recorded spectral data from them using an Ocean Optics S2000 Spectrometer (range of 250–880 nm, Dunedin, FL, USA) and a UV (deuterium bulb) and a visible (tungsten–halogen bulb) light source. We used a bifurcated fibre-optic measuring probe (Ocean Optics), which provided illumination from the lamp and transferred light reflected from the feather sample back to the spectrometer. This probe was held at a 90° angle to the feather surface. Ambient light was excluded with a block sheath that held the probe tip at a fixed distance of 5 mm from the feather surface, providing a reading area of 2 mm. All reflectance data were generated relative to a white standard (WS-1, Ocean Optics, Dunedin, FL, USA). We used OOIBase software to record 20 spectra sequentially and average them. The probe was lifted and replaced, and a new measurement taken, five times on each feather sample. We then averaged these five measurements for each sample.

We calculated indices for three different elements of colour from these reflectance spectra (Hailman 1977). These indices were restricted to wavelengths between 300 and 700 nm as evidence suggests that passerine birds are sensitive to UV wavelengths (300–400 nm; Cuthill *et al.* 2000) and that 700 nm is the upper limit of the vertebrate visual system (Jacobs 1981).

*Author for correspondence (shawkmd@auburn.edu).
† Present address: Department of Ecology and Evolutionary Biology, University of Arizona, 310 BioScience West, Tucson, AZ 85721, USA.
†The first two authors contributed in equal part to this work.

Table 1. Means, standard deviations and coefficients of variation of colour variables and nanostructural elements of eastern bluebird feather barb spongy layer.

	colour				nanostructure					
variable	hue (nm)	brightness	spectral saturation (%)	UV–violet chroma (%)	number of circular keratin rods	circular keratin rod diameter (nm)	number of circular air spaces	circular air space diameter (nm)	irregular keratin rod width (nm)	irregular air space width (nm)
mean	410.80	8232.69	23.00	44.00	31.83	48.25	31.29	51.32	45.47	59.62
± 1 s.e.m.	2.50	1128.37	0.30	0.70	3.12	1.58	2.46	1.76	1.35	2.45
CV	2.10	13.70	4.56	5.67	33.90	11.30	27.30	11.90	10.30	14.22

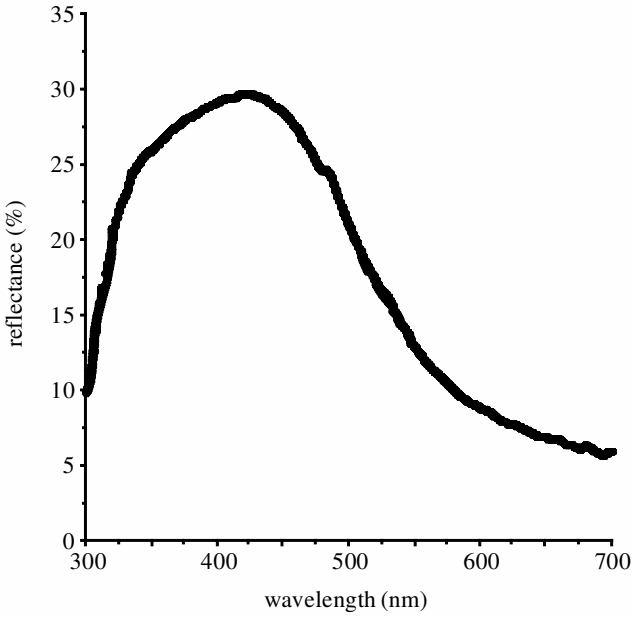

Figure 1. Typical reflectance spectra of rump feathers from a male eastern bluebird.

We measured hue, or the principal colour reflected by the feather, as the wavelength of peak reflectance. This measurement is a commonly used index of spectral location (e.g. Keyser & Hill 1999; Sheldon *et al.* 1999). Brightness, or the total amount of light reflected by the feather, was measured as the summed reflectance from 300–700 nm (Endler 1990; Andersson 1999). Chroma, or spectral purity, was measured in two ways. We measured UV–violet (UV–V) chroma as the proportion of UV–V light (i.e. 300–420 nm) reflected. However, this measurement is highly correlated with hue. This correlation is caused by the dependence of the amount of light reflected in the UV on the wavelength of peak reflectance. Feathers with peak reflectance shifted towards the UV will necessarily reflect more light within the range over which UV–V chroma is calculated. To decouple these variables, we also measured 'spectral saturation' as the proportion of light reflected within a range of 50 nm on either side of the hue value. We selected 12 males from the 30 males for which we had plumage colour data. These 12 males spanned the natural range of colour variation in the population.

(c) *Microscopy*

We cut feather barbs from the upper 1 cm of contour feathers and incubated them in 0.25 M sodium hydroxide and 0.1% Tween-20 for 30 min on a bench-top shaker. These barbs were then changed into 2 : 3 (v/v) of formic acid and ethanol for 2.5 h. Feather barbs were dehydrated by incubating in 100% ethanol twice and 100% propylene oxide once, and infiltrated with Epon in successive concentrations of 15, 50, 70 and 100%. Each of these infiltration steps was performed under vacuum in a desiccator for 24–48 h. Barbs were placed into moulds with the most distal tip of the barb at the top of the mould, and then the blocks were cured in an oven at 20 °C for 24 h. Barbs were cut using a diamond knife on an RMC MT-X (Boeckeler Instruments, Tucson, AZ, USA) ultramicrotome. Sections were placed on a 200 mesh copper grid (EMS, Fort Washington, PA, USA) with Formvar support, post-stained in osmium and lead citrate, and viewed on a Phillips EM301 (Veeco FEI Inc, Hillsboro, OR, USA) at × 25 000 magnification. All micrographs ($n = 3$ or 4 barbs for each bird) of the spongy layer were taken at the most distal tip of the barb, directly under the cortex, but away from cell margins. We took micrographs of a waffle-pattern diffraction grating (Ted Pella, Redding, CA, USA) accurate to 1 nm ± 5% at the same magnification for calibration of the images.

TEM micrograph negatives were scanned at 400 d.p.i. using an Epson Perfection 1240U flatbed scanner, and analysed using the Scanning Probe Image Processor (SPIP) v. 2.3.1 (Image Metrology 2002).

(d) *Fourier analysis*

We analysed these images using methods of Fourier analysis similar to those of Prum *et al.* (1998, 1999*a*). We wanted to determine if the nanostructure of bluebird feather barbs was sufficiently organized to produce colour by coherent light scattering, and if variation in the organization of this tissue explained variation in hue (for a more detailed explanation of Fourier analysis, see Prum *et al.* (1999*a*)).

To perform Fourier analysis, micrographs were first calibrated against the waffle-pattern diffraction grating in SPIP. We selected a 1024 pixel × 1024 pixel section of pure spongy layer from these calibrated images, avoiding the cortex and any cell boundaries or melanin granules. To correct for nonlinear coupling between the lateral plane and the z-axis in the image, we flattened the image by applying a least mean-square plane correction (Image Metrology 2002) to each section. The mean refractive index (MRI) of each section was estimated using 2-bin histograms of the frequency of dark (air) and light (keratin) pixels and the estimated refractive indices of keratin (RI = 1.54) and air (RI = 1.00) (Dyck 1971*b*).

The 2D fast Fourier transform (FFT) module of SPIP was used to create 2D Fourier power spectra for each image. The

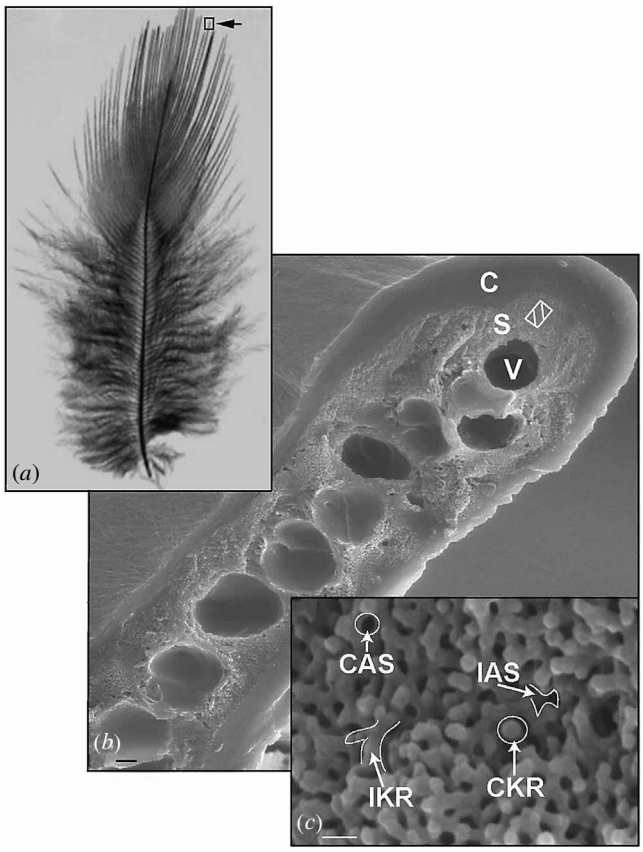

Figure 2. (*a*) A rump feather from a male eastern bluebird. The box around the tip of the barb indicates the region sectioned for SEM and TEM examination. (*b*) SEM (× 1000) of barb cross-section. The hatched box at the most distal region of the barb is enlarged in (*c*). Scale bar, 4 μm. (*c*) SEM (× 20 000) of the spongy region (S) directly under the cortex (C), but above the vacuoles (V) of the feather barb. The nanostructural components outlined include an irregular keratin rod (IKR), circular keratin rod (CKR), irregular air space (IAS) and circular air space (CAS). Scale bar, 80 nm.

radial spectra were then calculated using the roughness module of SPIP. These radial spectra exhibited two to four discrete peaks varying in strength. We multiplied each peak by twice the MRI for the tissue, resulting in several predicted hue values for each image. Frequently, the value resulting from the strongest peak for each image was outside the visual spectra of vertebrates, probably because of the inherent background 'noise' of most biological tissues (J. Jorgensen, personal communication). Thus, we selected the value resulting from the strongest peak within the visible spectrum. The values we obtained were close to those obtained from the same images ($n = 2$) using Prum *et al.*'s (1998, 1999*a*) techniques (R. O. Prum, personal communication). We averaged the Fourier-predicted hues from the images for each bird and compared them with those measured using spectrometry.

(e) *Nanostructural variation*

We measured the diameter of all circular keratin rods and air spaces within the selected area of pure keratin using the segment analysis tool of SPIP. Using this same tool, we measured the mean width of all irregular keratin rods and air spaces. All measurements were performed by one author (M.D.S.). We tested the repeatability of these measurements by performing them three times on all images. Repeatability was high for both irregular ($R = 0.945$ for air spaces, $R = 0.930$ for keratin rods) and circular ($R = 0.855$ for air spaces, $R = 0.801$ for rods) elements. To estimate the diameter of the 'hollow cylinders' (circular air spaces surrounded by keratin rods), we added twice the mean width of the irregular keratin rods to the mean diameter of the circular air spaces (Dyck 1971*b*). We calculated the mean of each nanostructural element for each image and then the mean of all images for each bird.

(f) *Statistical analyses*

All analyses were performed on SPSS v. 10.0 for Macintosh (SPSS 2001). We performed stepwise linear regressions using number, diameter and standard error of diameter of circular keratin rods and air spaces, diameter of hollow cylinders and mean width and standard error of keratin and air bars as independent variables. Hue, total brightness, UV–V chroma and spectral saturation were the dependent variables.

3. RESULTS

(a) *Spectrometry*

All feathers reflected most strongly in the UV–blue regions of the spectrum (table 1; figure 1). Variation was highest in total brightness and lowest in hue (table 1). UV–V chroma was significantly negatively correlated with hue (Spearman's rank correlation; $r_s = -0.902$, $p < 0.001$, $n = 12$ samples) and significantly positively correlated with spectral saturation ($r_s = 0.825$, $p = 0.001$, $n = 12$). Spectral saturation was significantly negatively correlated with hue ($r_s = -0.741$, $p = 0.006$, $n = 12$). None of the other colour variables was significantly correlated.

(b) *Microscopy*

The spongy layer of eastern bluebird feather barbs lies beneath a keratin cortex and above a layer of melanin granules surrounding large central vacuoles (figures 2*b* and 3*a*). This spongy layer is characterized by irregularly bent, as well as more circular, keratin rods and air spaces (figures 2*c* and 3*a*).

(c) *Fourier analysis*

All feather barbs showed discrete rings in the Fourier power spectra (figure 3*b*), indicating a high degree of uniformity and organization on a nanostructural scale (Vaezy & Clark 1994; Prum *et al.* 1998, 1999*a*,*b*).

The hue values predicted by Fourier analysis and those measured with a spectrometer on the same feathers were not correlated ($r_s = 0.126$, $p = 0.697$, $n = 12$; figure 4). The predicted and observed values deviated from one another by values ranging from 10 to 116 nm.

(d) *Nanostructural variation*

The number of circular keratin rods significantly predicted hue (stepwise linear regression, $\beta = 0.680$, $r^2 = 0.458$, $F_{1,11} = 8.581$, $p = 0.016$), and UV–V chroma ($\beta = -0.677$, $r^2 = 0.462$, $F_{1,11} = 8.466$, $p = 0.016$; figure 5*a*). Because these two colour variables are not independent, we performed a stepwise linear regression with number of keratin rods as the dependent variable and hue and UV–V chroma as independent variables. Only UV–V chroma was significantly predicted by the number of kera-

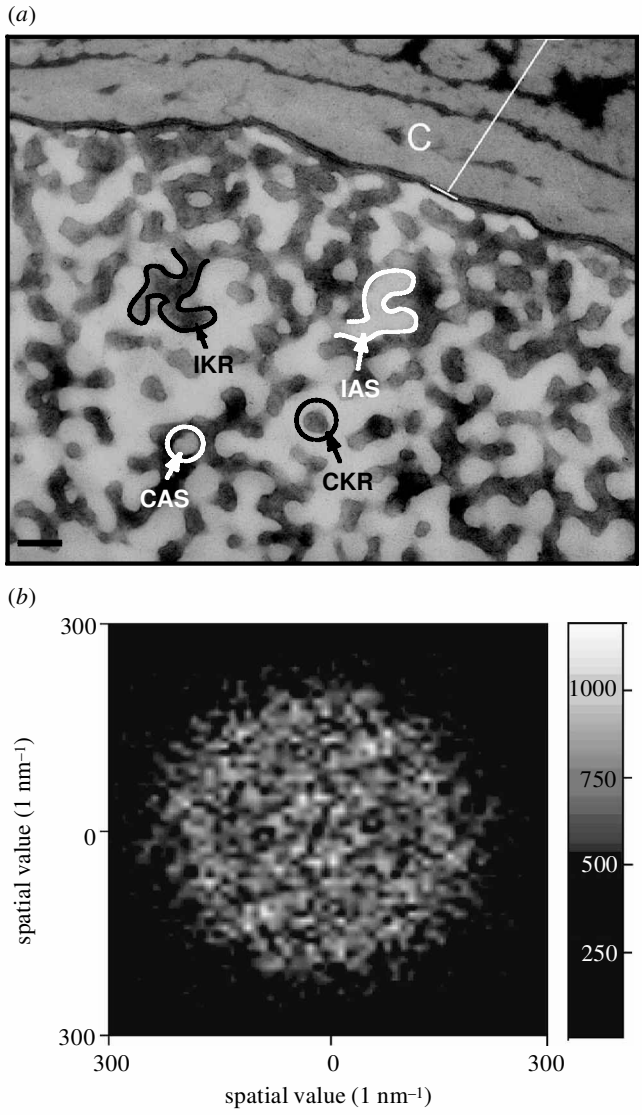

Figure 3. (*a*) Transmission electron micrograph (× 25 000) of the spongy layer of a contour feather from a male eastern bluebird. Abbreviations: C, cortex; IKR, irregular keratin rod; IAS, irregular air space; CKR, circular keratin rod; CAS, circular air space. Scale bar, 100 nm. (*b*) Two-dimensional Fourier power spectrum of TEM of colour-producing spongy layers of eastern bluebirds. The length and direction, respectively, of a vector from the origin to each value in the power spectrum indicates its spatial frequency and direction (for more details, see Prum et al. 1999*a*). The colour indicates the magnitude of each value in the power spectrum (scale on right).

tin rods ($r^2 = 0.462$, $p = 0.016$). The standard error of the diameter of circular keratin rods significantly predicted spectral saturation ($\beta = -0.706$, $r^2 = 0.498$, $F_{1,11} = 9.930$, $p = 0.010$; figure 5*b*). No variable significantly predicted total brightness.

4. DISCUSSION

The discrete rings that we observed in the Fourier power spectra demonstrate that colour production in this species is caused primarily by coherent light scattering owing to a nanostructural arrangement of keratin and air in the feather barbs (Prum *et al.* 1998, 1999*a*,*b*). These

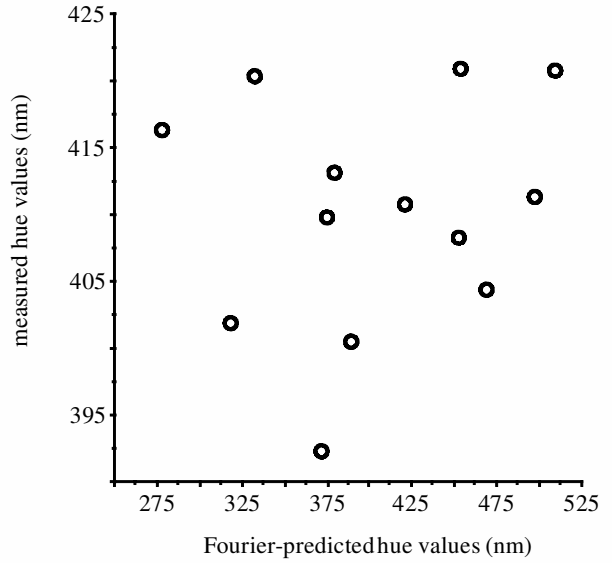

Figure 4. Scatterplot of the average hue (nm) of feathers of male eastern bluebirds, as predicted by Fourier analysis and as measured by spectrometry. $r_s = 0.126$, $p = 0.697$, $n = 12$.

rings are comparable with those found in other ordered tissue such as the caruncles of Malagasy asities (Prum *et al.* 1999*b*), the human sclera (Vaezy & Clark 1994), and barbs of birds such as the plum-throated cotinga (*Cotinga mayana*) (Prum *et al.* 1998) and the rose-faced lovebird (*Agapornis rosiecollis*) (Prum *et al.* 1999*a*). They show that the nanostructure is uniform in all directions. Fourier analysis allowed us to confirm that the nanostructure of bluebird feathers is ordered, but it did not successfully predict the hue of individual birds.

Fourier analysis of micrographs of the spongy layer appears to lack the resolution to accurately predict the small-scale variation we observed. Previously reported Fourier-predicted hue values have been from 0 to 75 nm away from measured values for feather barbs (Prum *et al.* 1998, 1999*a*), and up to 117 nm away from measured values for other tissues (Prum *et al.* 1999*b*). Resolution could be improved, and error could be reduced, by increasing the number of micrographs examined for each barb (Prum *et al.* 1999*b*; R. O. Prum, personal communication), but Fourier analysis is probably more useful for comparing large-scale differences in colour between species (see, for example, Prum *et al.* 1998, 1999*a*) than small-scale differences within species.

Although our efforts to predict intraspecific variation in hue using Fourier analysis were unsuccessful, we found that morphological variables within the spongy layer predicted variation in colour quite well. The standard error of the diameter of circular keratin rods strongly predicted spectral saturation, whereas the number of circular keratin rods strongly predicted UV–V chroma. The negative relation between the amount of variation in the diameter of keratin rods and the purity of the reflected colour suggests that the precision of the nanostructural elements determines spectral saturation, as has been speculated by some authors (Fitzpatrick 1998; Andersson 1999; Keyser & Hill 1999). When elements are uniform in size, the reflected light will be tightly grouped around the wavelength of peak reflectance. Increasing the variation in those elements may break up this tight grouping and spread the

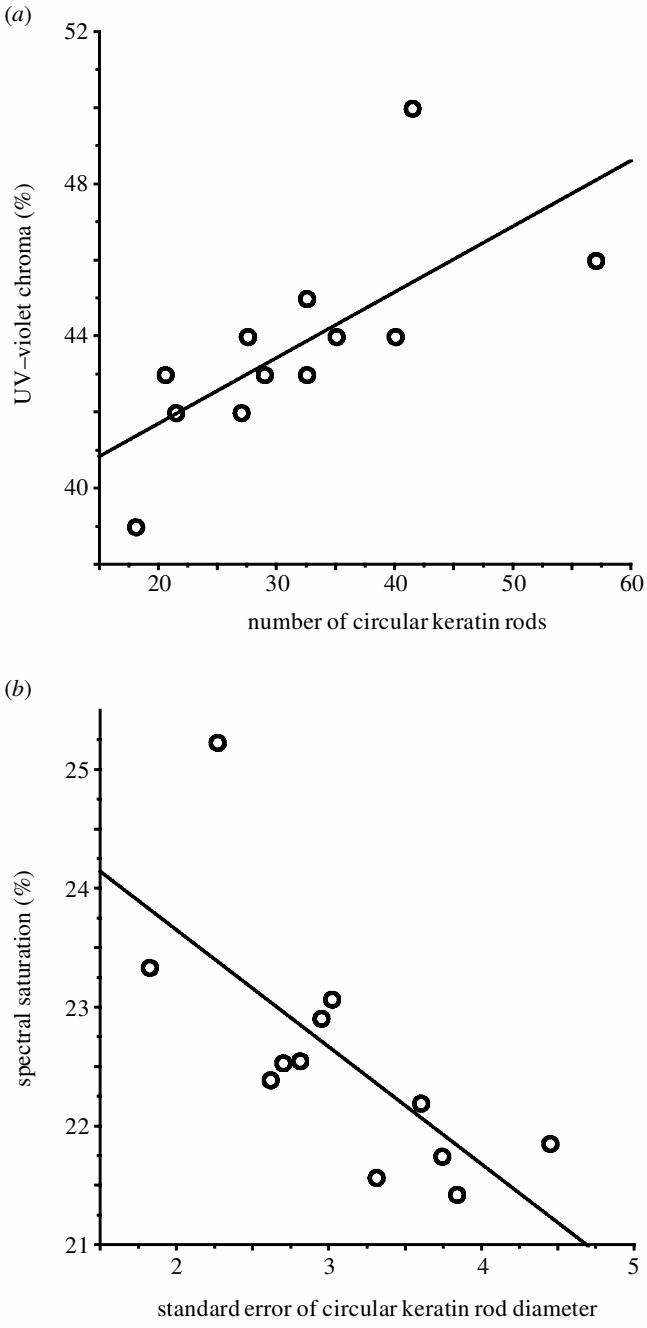

Figure 5. Scatterplots of colour variables versus nanostructural variables of feather barbs from male eastern bluebirds. Colour was measured from intact feathers, whereas nanostructure was measured from 1024 pixel × 1024 pixel sections of TEM micrographs of the barbs' spongy layer. (*a*) Scatterplot of UV–V chroma versus the number of circular keratin rods. (*b*) Scatterplot of spectral saturation versus the standard error of circular keratin rod diameter. Stepwise linear regressions: (*a*) $r^2 = 0.462$, $p = 0.016$. (*b*) $r^2 = 0.498$, $p = 0.010$. $n = 12$ in all cases.

reflected light over a broader spectrum. To our knowledge, this is the first demonstration of a possible mechanism for intraspecific variation in UV–blue structural colour. However, a link between condition at the time of feather growth and size and uniformity of feather elements has yet to be demonstrated.

Both coherent (Benedek 1971) and incoherent (Kerker *et al.* 1966; Kerker 1969; Finger 1995) models of colour production predict positive relations between number of scattering elements and intensity (brightness) of the reflected light. The number of circular keratin rods in our study predicted relative brightness in the UV–V range, but not overall brightness. This effect could be restricted to this range because other factors such as thickness of the keratin cortex alter total brightness (see below). In any case, the highly ordered nanostructure of these barbs argues strongly against Rayleigh and Mie scattering as the basis of colour production. Models of coherent scattering are more likely to explain this relation.

Other colour variables were not significantly related to the structural elements of feathers that we measured. Between species, hue is generally positively associated with the size of keratin and/or air elements (Dyck 1971*b*, 1976; Finger *et al.* 1992; Finger 1995). In our comparisons of male eastern bluebirds, hue was not positively associated with the size of any structural elements, but hue was the least variant of our colour measurements (see table 1). We may need larger sample sizes to discern the effects of structural element size on hue. The relation between hue and number of keratin rods appears to be caused by the tight correlation between hue and UV–V chroma.

Variation in total brightness was not explained by our data and may be caused by morphological features outside the spongy layer. Variables such as the thickness of the keratin cortex (Finger 1995; Andersson 1999), the abundance of heavily melanized barbules (Andersson 1999) or the number of melanin granules within the spongy layer itself (A. M. Estes and M. D. Shawkey, personal observation) may affect brightness. As brightness has been shown to play an important part in sexual signalling (Hunt *et al.* 1999; Doucet & Montgomerie 2003), understanding the mechanisms by which it varies should be a high priority for future research.

Recent work suggests that structural plumage colour may serve as an honest, sexually selected signal (Andersson *et al.* 1998; Bennett *et al.* 1997; Keyser & Hill 1999; Sheldon *et al.* 1999; Siefferman & Hill 2003). We have shown that the precision of structural elements determines the spectral saturation of colour. These results suggest that the honesty of structural signals may be maintained by the cost of accurately producing them (handicap model; Zahavi 1975). Alternatively, the tightly constrained physiological processes involved in their production may make them necessarily 'honest' (revealing indicator model; Iwasa *et al.* 1991). Genetic differences between individuals may also cause differences in colour. Future work should focus on whether the precise nanostructure responsible for bright structural plumage characteristics is energetically costly to produce.

The authors are grateful to M. Toivio-Kinnucan at the Auburn University Veterinary School for preparing feather barbs for microscopy. J. Jorgensen (Image Metrology) helped with image analysis, and S. Reeves improved the authors' understanding of Fourier analysis. R. O. Prum analysed some images, and answered questions about Fourier analysis. R. Dute assisted with SEM in an earlier version of this project. R. Montgomerie allowed the use of his programs for calculating spectral data. This manuscript was improved by comments from M. L. Beck, S. M. Doucet, K. L. Farmer, D. P. Mennill and P. M. Nolan. This work was funded in part by NSF grants DEB007804 and IBN9722971 (both to G.E.H.).

REFERENCES

Andersson, S. 1999 Morphology of UV reflectance in a whistling-thrush: implications for sexual selection. *J. Avian Biol.* **30**, 193–204.

Andersson, S., Örnborg, J. & Andersson, M. 1998 Ultraviolet sexual dimorphism and assortative mating in blue tits. *Proc. R. Soc. Lond.* B **265**, 445–450. (DOI 10.1098/rspb.1998.0315.)

Benedek, G. B. 1971 Theory of transparency of the eye. *Appl. Optics* **10**, 459–473.

Bennett, A. T. D., Cuthill, I. C., Partridge, J. C. & Lunau, K. 1997 Ultraviolet plumage colours predict mate preferences in starlings. *Proc. Natl Acad. Sci. USA* **94**, 8618–8621.

Cuthill, I. C., Partridge, J. C., Bennett, A. T. D., Church, S. C., Hart, N. S. & Hunt, S. 2000 Ultraviolet vision in birds. *Adv. Stud. Behav.* **29**, 159–215.

Doucet, S. M. & Montgomerie, R. 2003 Multiple sexual ornaments in satin bowerbirds: UV plumage and bowers signal different aspects of male quality. *Behav. Ecol.* (In the press.)

Dyck, J. 1971*a* Structure and colour-production of the blue barbs of *Aganorpis roseicollis* and *Cotinga maynana*. *Z. Zellforsch.* **115**, 17–29.

Dyck, J. 1971*b* Structure and spectral reflectance of green and blue feathers of the lovebird (*Aganorpis roseicollis*). *Biol. Skr.* **18**, 1–67.

Dyck, J. 1976 Structural colours. *Proc. Int. Ornithol. Congr.* **16**, 426–437.

Endler, J. A. 1990 On the measurement and classification of colour in studies of animal colour patterns. *Biol. J. Linn. Soc.* **41**, 315–352.

Finger, E. 1995 Visible and UV coloration in birds: Mie scattering as the basis of color production in many bird feathers. *Naturwissenschaften* **82**, 570–573.

Finger, E., Burkhardt, D. & Dyck, J. 1992 Avian plumage colors: origin of UV reflection in a black parrot. *Naturwissenschaften* **79**, 187–188.

Fitzpatrick, S. 1998 Colour schemes for birds: structural coloration and signals of quality in feathers. *Ann. Zool. Fenn.* **35**, 67–77.

Gadow, H. 1882 On the colour of feathers as effected by their structure. *Proc. Zool. Soc. Lond.* 409–421.

Häcker, V. & Meyer, G. 1902 Die blaue farbe der Voelfedern. *Zool. Jb. Abt. Syst. Geog. Biol. Tiere* **15**, 267–294.

Hailman, J. P. 1977 *Optical signals*. Bloomington, IN: Indiana University Press.

Hunt, S., Cuthill, I. C., Bennett, A. T. D. & Griffiths, R. 1999 Preferences for ultraviolet partners in the blue tit. *Anim. Behav.* **58**, 809–815.

Image Metrology 2002 *The Scanning Probe Image Processor*. Denmark: Lyngby.

Iwasa, Y., Pomiankowski, A. & Nee, S. 1991 The evolution of costly male preferences. II. The 'handicap' principle. *Evolution* **45**, 1431–1442.

Jacobs, G. H. 1981 *Comparative color vision*. New York: Academic Press.

Kerker, M. 1969 *The scattering of light and other electromagnetic radiation*. New York: Academic Press.

Kerker, M., Farone, W. A. & Jacobsen, R. T. 1966 Color effects in the scattering of white light by micron and submicron spheres. *J. Opt. Soc. Am.* **56**, 1248–1255.

Keyser, A. J. & Hill, G. E. 1999 Condition-dependent variation in the blue-ultraviolet colouration of a structurally based plumage ornament. *Proc. R. Soc. Lond.* B **266**, 771–777. (DOI 10.1098/rspb.1999.0704.)

Prum, R. O. 1999 The anatomy and physics of avian structural colors. *Proc. Int. Ornithol. Congr.* **22**, 1–22.

Prum, R. O., Torres, R. H., Williamson, S. & Dyck, J. 1998 Constructive interference of light by blue feather barbs. *Nature* **396**, 28–29.

Prum, R. O., Torres, R. H., Williamson, S. & Dyck, J. 1999 Two-dimensional Fourier analysis of the spongy medullary keratin of structurally coloured feather barbs. *Proc. R. Soc. Lond.* B **266**, 13–22. (DOI 10.1098/rspb.1999.0598.)

Prum, R. O., Torres, R. H., Kovach, C., Williamson, S. & Goodman, S. M. 1999*b* Coherent light scattering by nanostructured collagen arrays in the caruncles of Malagasy asities. *J. Exp. Biol.* **202**, 3507–3522.

Sheldon, B. C., Andersson, S., Griffith, S. C., Örnborg, J. & Sendecka, J. 1999 Ultraviolet colour variation influences blue tit sex ratios. *Nature* **402**, 874–877.

Siefferman, L. M. & Hill, G. E. 2003 Structural and phaeomelanin coloration indicate parental effort and reproductive success in male eastern bluebirds. *Behav. Ecol.* (In the press.)

SPSS 2001 SPSS 10.0 for Macintosh. Chicago, IL: SPSS.

Vaezy, D. & Clark, J. I. 1994 Quantitative analysis of the microstructure of the human cornea and sclera using 2-D Fourier methods. *J. Microsc.* **175**, 93–99.

Zahavi, A. 1975 Mate selection—a selection for a handicap. *J. Theor. Biol.* **53**, 204–214.